Terahertz lasers based on intracentre transitions of group V donors in uniaxially deformed silicon

K.A. Kovalevsky, N.V. Abrosimov, R.Kh. Zhukavin, S.G. Pavlov, H.-W. Hübers, V.V. Tsyplenkov, V.N. Shastin

Abstract. **This paper presents a brief overview of available experimental data on the characteristics of stimulated terahertz emission (4.9–6.4 THz) from optically excited neutral group V donors (phosphorus, antimony, arsenic and bismuth) in crystalline silicon subjected to uniaxial compressive strain along the [100] axis. Strain is shown to have a significant effect on the characteristics in question. Optimal strain depends on the dopant and may reduce the threshold pump intensity and improve lasing efficiency. We discuss possible mechanisms behind this effect and estimate the limiting output emission parameters.**

Keywords: silicon laser, uniaxial deformation, terahertz radiation.

1. Introduction

The possibility of long-wavelength IR emission on intracentre transitions of donors and acceptors in silicon under optical excitation was first demonstrated in 1996 [1]. Four years later, the effect was observed upon optical excitation of phosphorus donors in liquid helium-cooled silicon by TEA CO_2 laser radiation [2]. Some time later, similar results were obtained with other group V donors (Sb, As and Bi) [3, 4]. The specifics of stimulated emission from such centres under intracentre optical excitation was investigated using a free-electron laser (FELIX). Changes in pump frequency were found to cause working transition switching, and lasing due to Stokes-shifted Raman scattering from donor-bound electrons was demonstrated [5–9]. The subject of most studies has been undeformed silicon. Measurement results made it possible to identify working transitions, optimise the doping level [$(2-4) \times 10^{15}$ cm^{-3}],

K.A. Kovalevsky, R.Kh. Zhukavin, V.V. Tsyplenkov Institute for Physics of Microstructures, Russian Academy of Sciences, Akademicheskaya ul. 7, 607680 der. Afonino, Kstovskii raion, Nizhnii Novgorod region, Russia; e-mail: atan4@yandex.ru, zhur@ipmras.ru;
N.V. Abrosimov Institute for Crystal Growth, Max-Born-Strasse 2, 12489 Berlin, Germany;
S.G. Pavlov Institute of Planetary Research, German Aerospace Center (DLA), Rutherfordstrasse 2, 12489 Berlin, Germany;
H.-W. Hübers Institute of Planetary Research, German Aerospace Center (DLA), Rutherfordstrasse 2, 12489 Berlin, Germany; Institute für Optik und Atomare Physik, Technische Universität Berlin, Strasse des 17 Juni 135, 10623 Berlin, Germany;
V.N. Shastin N.I. Lobachevski Nizhnii Novgorod State University, prosp. Gagarina 23, 603950 Nizhnii Novgorod, Russia; Institute for Physics of Microstructures, Russian Academy of Sciences, Akademicheskaya ul. 7, 607680 der. Afonino, Kstovskii raion, Nizhnii Novgorod region, Russia; e-mail: shastin@ipmras.ru

evaluate possible gain coefficients (0.1–0.2 cm^{-1}) and determine limiting working temperatures (15--25 K) and threshold pump intensities (30 kW cm^{-2} for P and Sb and 300 kW cm^{-2} for As and Bi) [10]. The decay rate was estimated for the most important states [11, 12].

Uniaxial deformation of a crystal produces significant changes in conduction band states, which tells on relaxation processes and the population of working states and changes the polarisation characteristics of the medium. This paper presents a review of results obtained to date on stimulated emission from optically excited donors in uniaxially deformed silicon upon compression along the [100] axis.

2. Uniaxial deformation

It is known that silicon has six identical but differently oriented X-valleys in the conduction band and that the effective mass approximation adequately describes all odd excited states ($2p_0$, $2p_\pm$, $3p_0$ and others) of donors. Such states are produced independently at each valley and are thus sixfold degenerate. This is, however, not so in the case of even states (1s, 2s and others). The incorporation of a dopant into a silicon site results in a local distortion of the crystal lattice and produces a unit-cell-scale potential (unit-cell potential). The additional potential splits the even states and partially lifts their degeneracy. The states of the six valleys then intermix with each other to form an A_1 singlet, E doublet and T_2 triplet. The notations A_1, E and T_2 reflect the symmetry of states and correspond to the irreducible representations of T_d (tetrahedron) point-group symmetry [13, 14]. This refers primarily to the most localised state 1s, which splits into 1s(A_1), 1s(E) and 1s(T_2). The energies of the 1s(E) and 1s(T_2) states differ by ~1 meV and approach the energy of the ground state of a 'pure' Coulomb centre (31.3 meV). At the same time, the correction Δ to the energy of the 1s(A_1) ground state is rather large: 11.4, 14.3, 22.5 and 39.7 meV for the Sb, P, As and Bi donors, respectively. It is commonly referred to as a chemical shift. In addition, spectra of the antimony in Si:Sb and the bismuth in Si:Bi demonstrate a splitting of the 1s(T_2) state into 1s(T_2:Γ_7) and 1s(T_2:Γ_8), related to the spin–orbit coupling potential (we use notations from Mayur et al. [15]). Bi has the largest Λ_{so} splitting: $\Lambda_{so} \approx 0.71$ meV [16] (for example, Sb has $\Lambda_{so} \approx 0.29$ meV [15]). In the case of P and As centres, the effect of spin–orbit coupling is negligible.

On the other hand, uniaxial deformation of a crystal also reduces the degeneracy and splitting δE of the states of the differently oriented conduction band valleys. Figure 1 shows typical dependences of the energy of conduction band states on uniaxial compressive strain along the [100] axis for Si:P ($\Lambda_{so} = 0$) and Si:Bi ($\Lambda_{so} = 0.71$ meV). The symbols of
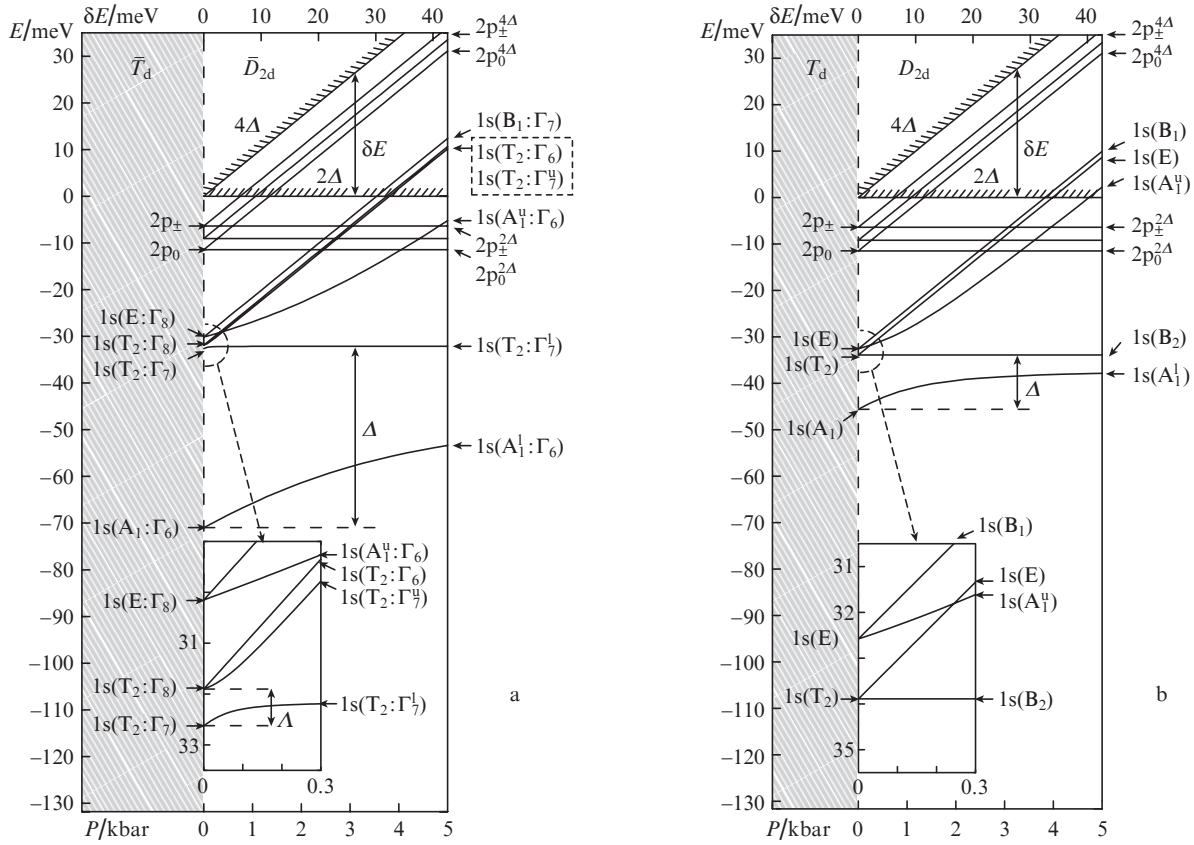
Figure 1. Energy level diagram of electron states in (a) Si : Bi and (b) Si : P for compressive uniaxial deformation of a silicon crystal; $F \parallel [100]$.

states in the 1s group have superscripts (l = lower and u = upper) that specify their relative position on the energy axis. The superscripts 2Δ and 4Δ specify that the states belong to the 2Δ and 4Δ valleys, respectively. It is worth noting that, for $\delta E \gg \Delta$, the unit-cell potential does not couple the 1s states of the 2Δ and 4Δ valleys. For the triplet states, the hybridisation of these valleys due to the spin–orbit coupling is suppressed even for $\delta E > \Lambda_{so}$. The splitting δE is related to pressure P by $\delta E = \Xi_u(s_{11} - s_{12})P$. Here $\Xi_u = 8.77$ eV is the deformation potential constant and $s_{11} - s_{12} = 9.7 \times 10^{-12}$ Pa^{-1} are stiffness tensor components [14].

In the case of undeformed silicon pumped by a CO_2 laser, an inverted distribution results from the accumulation of photo-excited electrons at long-lived 2p states (Fig. 2). The lower working levels are the group of 1s(E) and 1s(T_2) split-off states. In the case of the Sb and P donors, the working transitions are $2p_0 \to 1s(T_2)$; those for As and Bi are $2p_\pm \to 1s(E)$ and $2p_\pm \to 1s(T_2)$. Changes in conduction band states influence the relaxation of excited electrons, the population of working states and stimulated emission. Note the most important factors. First, at a sufficiently high strain along the [100] axis, electrons excited into the conduction band are then not distributed over the six valleys but relax predominantly to the lower 2Δ valleys. For $e_0 \parallel F$, where e_0 is the wave field vector and F is the compressive force acting on the crystal, this ensures the highest possible gain on the $2p_0^{2\Delta} \to 1s^{2\Delta}$ optical transition. For comparison, at $\delta E = 0$ only one-third of the electrons effectively contribute to the gain (Fig. 3). Note that deformation of the crystal changes the photoionisation cross section σ of the centre. According to the ground state wave function of a donor at a [100] strain $\delta E > \Delta$ [13] under pumping by a CO_2 laser
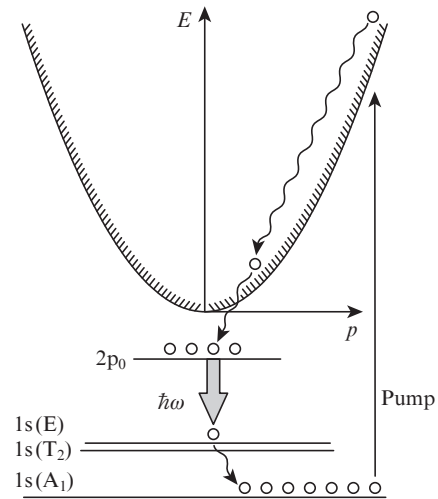

Figure 2. Schematic of the formation of population inversion between states of phosphorus (P), a shallow donor in silicon (Si), in momentum space under photoexcitation by a CO_2 laser.

(~ 10.6 μm), with increasing stress $\sigma \to \sigma_\perp$ ($\sim 4/3 \sigma_0$) for $e \perp F$ and $\sigma \to \sigma_\parallel$ ($\sim 1/4 \sigma_0$) for $e \parallel F$, where σ_0 is the photoionisation cross section in undeformed silicon; e is the pump field vector; and $\sigma_\perp$ and $\sigma_\parallel$ are the photoionisation cross sections for one valley in the ground state at pump field polarisations across and along the heavy mass, respectively. In our estimates, we used the $\sigma_\perp$ и $\sigma_\parallel$ values from Ref. [17]. Thus, with increasing strain, optical pumping with $e \perp F$ becomes somewhat more effective.
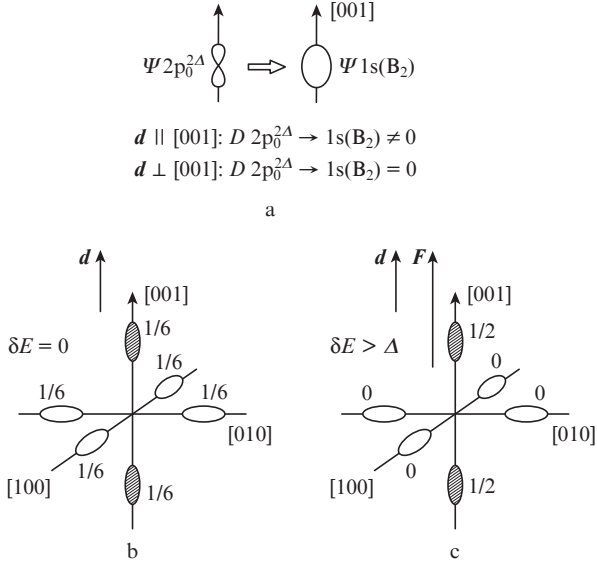
Figure 3. $2p_0 \rightarrow 1s$ optical transition in silicon: (a) wave functions Ψ and matrix element D of the dipole transition; (b,c) population of the valleys in undeformed ($\delta E = 0$) and uniaxially deformed ($\delta E > \Delta$) silicon, respectively. The numbers (0, 1/6 and 1/2) specify the electron distribution over the valleys. The hatched valleys have nonzero matrix elements for the indicated vector d.

Another distinctive feature of a uniaxially deformed crystal is a change in the state of negatively charged donors (D⁻ centres), which result from partial ionisation of the dopant. They absorb radiation in a wide range of THz frequencies and produce considerable internal losses. According to theory and measurements, the binding energy of a D⁻ centre decreases from 2 to ~0.5 meV with increasing strain [18]. At an electron temperature $T \approx 10$ K, this should lead to a considerable decrease (by about a factor of 10) in electron concentration N (Fig. 4) and to the associated absorption. To verify this conclusion, the absorption of THz radiation by optically excited donors in a silicon crystal was measured as a function of strain. Along with a CO_2 laser, a quantum cascade laser ($\lambda = 97$ μm) was used as a probe source. The modulation of the quantum cascade laser beam after it passed through Si:As

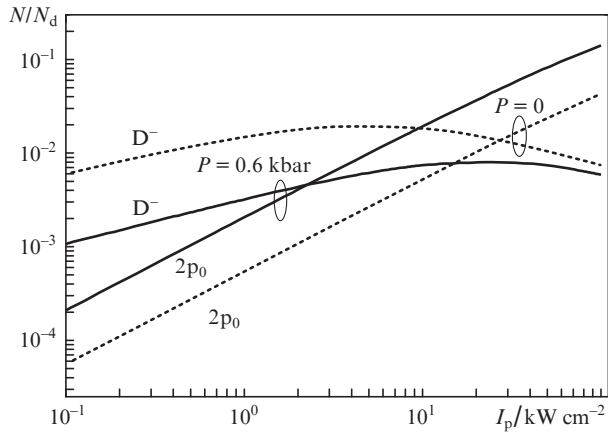and Si:Bi samples exposed to a CO_2 laser beam was recorded using a Ge:Ga detector. The measurement results are presented in Fig. 5. According to our results, the absorption of THz radiation decreases by at least a factor 5 with decreasing strain for $P < 1$ kbar.
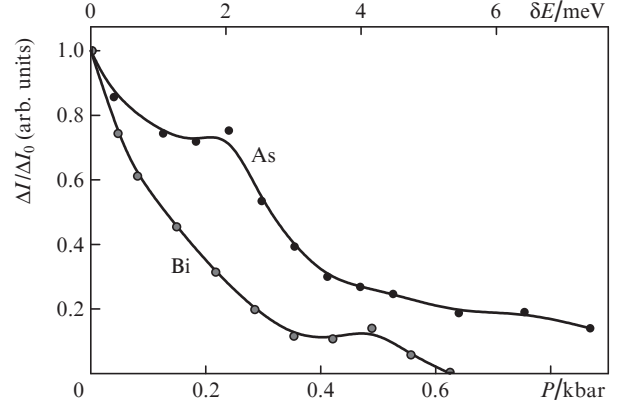

Figure 5. Absorption $\Delta I = \max(I_{in} - I_{out})$ normalised to $\Delta I_0 = \Delta I (P = 0)$ vs. [100] compressive strain for quantum cascade laser radiation ($\lambda = 97$ μm).

Yet another important factor is the change in the lifetime of working states in a uniaxially deformed crystal. For example, the relaxation of the upper working state $2p_0$ in P and Sb is controlled by the emission of LA-g and TA-f short-wavelength (intervalley) phonons, responsible for electron transitions between the valleys. It can be shown that even slight strain along the [100] axis prevents the decay of the $2p_0$ state to the $1s(B_2)$ state, assisted by TA-f intervalley phonons. According to calculations, the lifetime of the $2p_0$ state in uniaxially deformed silicon should increase two to three times [12].

Figure 6 presents calculation results for $\delta N/N_d$, which characterises the inverse population as a function of [100] compressive strain for working transitions of the phosphorus, arsenic and antimony donors in silicon under CO_2 laser excitation (unpolarised light) [19]. Here, δN is the population difference for the working transition indicated in Fig. 6 and N_d is the donor concentration. To evaluate populations, we

Figure 4. Calculated population inversion as a function of CO_2 laser pump intensity for $2p_0$ and D⁻ centres in Si:Sb. N_d is the donor concentration.
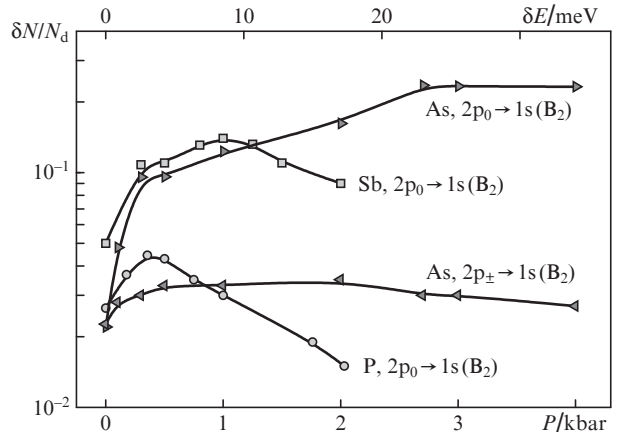

Figure 6. Population inversion as a function of strain ($F \parallel [100]$) for the $2p_0, 2p_\pm \rightarrow 1s(B_2)$ transitions of the Sb, P and As donors. δN is the population difference for the working transition.

solved a system of linear balance equations. The photoionisation rate was taken to be constant at $\sim 10^9$ s^{-1} and we used ideas of cascade electron capture at upper excited states of the donor and the emission of long-wavelength acoustic phonons [20]. The effect of strain on the relaxation rate of all important states was properly taken into account [12]. In our calculations, the distance between the centres of the valleys in the [100] direction was taken to be $K_0 = 0.835 \times 2\pi a^{-1}$, where a is the lattice parameter of the crystal. Note that K_0 was variously reported to be from $0.83 \times 2\pi a^{-1}$ to $0.85 \times 2\pi a^{-1}$ [21, 22]. The relevant electron–phonon interaction constants were taken from Ref. [21], but they are also not absolutely reliable. Nevertheless, despite the above-mentioned drawbacks, the theoretical curves in Fig. 6 help to identify the key factors influencing the effect of strain on stimulated emission intensity.

3. Silicon samples and experimental techniques

Silicon crystals were grown by the floating-zone technique and doped with group V donors to a concentration $N_d \approx 3 \times 10^{15}$ cm^{-3} ($N_a/N_d < 1\%$). Samples were cut in the form of parallelepipeds oriented in the [100] and [110] crystallographic directions. The dimensions and other parameters of the samples are given in Table 1. The faces of the samples were oriented to within 1′ accuracy and polished. As a result, each sample was a high-Q cavity for total internal reflection modes. THz radiation was coupled out owing to diffraction and/or departure of the faces from parallelism. According to test measurements, the losses in such resonators, including absorption by the crystal lattice, were within $0.01 - 0.02$ cm^{-1}. The compressive stress reached $4 - 5$ kbar and was applied along the long edge of the samples. The samples were pumped at a wavelength $\lambda = 10.6$ μm ($\hbar\omega = 117$ meV) by a Q-switched CO$_2$ laser. The pump field was normal to the deformation direction. The maximum pump intensity was ~ 4 kW cm^{-2}, at a pulse duration of ~ 300 ns. The samples were cooled by liquid helium. The experimental configuration is schematised in Fig. 7. The THz radiation was detected by a Ge:Ga photodetector. To prevent the pump radiation from reaching the

Table 1. Silicon samples studied.

Sample	Material	Dimensions/mm	$N_d/10^{15}$ cm^{-3}
1	Si:Sb	2.75×4.70×6.15	4
2	Si:P	2.75×4.90×6.20	4
3	Si:As	1.90×6.10×4.10	2
4	Si:Bi	2.55×4.90×6.00	3

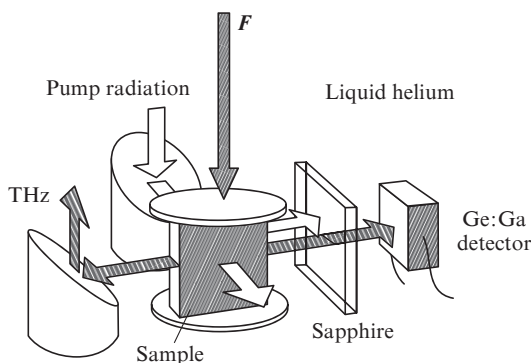Note: deformation along the [100] axis; float zone crystal growth.

Figure 7. Experimental configuration.

photodetector, we used a 1-mm-thick sapphire plate. Stimulated emission spectra were measured on a Fourier transform spectrometer with a resolution of ~ 0.2 cm^{-1}.

4. Experimental results

Figure 8 shows the measured output stimulated emission intensity as a function of uniaxial strain for all group V donors in silicon crystals compressed along the [100] axis. Analogous results, obtained under pumping by ~ 100-ns TEA CO$_2$ laser pulses, were reported previously [23 – 25]. It is seen that the use of 300-ns CO$_2$ laser pulses allows the threshold pump intensity for the P, Sb and As donors to be reduced to a level of ~ 100 W cm^{-2}, which is two orders of magnitude lower than that in undeformed silicon and a factor of $2 - 3$ lower than that under pumping by a TEA CO$_2$ laser.

For all donors, the output stimulated emission intensity is a nonmonotonic function of strain. At $P = 0$, there is no lasing. Laser action begins when P reaches a certain value. With increasing stress, the output signal for the Sb, P and As donors increases and reaches a maximum, before falling off. The optimal strain for stimulated emission increases with an increase in the chemical shift of the centre. The Bi donor stands out in that it has resonances near $\delta E = 17$ and 22 meV (Figs 8g, 8h). Figure 9 shows the threshold pump intensity as a function of strain in the [100] crystallographic direction for all four impurities. The data points are connected by fitting curves. It is seen that the minimum lasing threshold for each donor is observed in a pressure range, which can be referred to as the optimal strain range. Sb, P and As have similar minimum lasing thresholds: 100, 200 and 300 W cm^{-2}, respectively. The Bi donor again stands out, with a minimum lasing threshold near 3.6 kW cm^{-2}.

Figure 10 shows the stimulated emission spectra of the donors in silicon for characteristic compressive strain values in the [100] crystallographic direction. It is seen that the lasing frequency varies slightly from donor to donor. Moreover, the lasing frequency of all the donors except P depends on strain. Note that Fig. 10 indicates the transitions responsible for the stimulated emission. They were identified using theoretical predictions as to the effect of strain on the spectrum of donor states. Such data for the Bi donor are presented in Fig. 1a, and those for P, in Fig. 1b. The spectra are consistent with reported absorption spectra (see e.g. Ref. [14]). Since the emission from the Bi donor has a special nature, Fig. 11 shows a detailed dependence of the lasing frequency on [100] compressive strain for this centre.

The principal characteristics of lasers based on intracentre transitions of donors in deformed silicon under optical CO$_2$ laser excitation are summarised in Table 2. Some of them were obtained by measurements, and some (marked by asterisks) were estimated theoretically. The estimates took into account pump absorption by the crystal lattice and the reduction in pump efficiency for working states because of the scattering to nonworking states.

5. Discussion

Our measurements clearly demonstrate that [100] uniaxial deformation increases the gain coefficient for intracentre transitions of group V donors in silicon under optical CO$_2$ laser excitation. As a consequence, the quantum efficiency of the emission increases and the lasing threshold decreases. It is seen from the data in Figs 8a – 8d that the P and Sb donors are
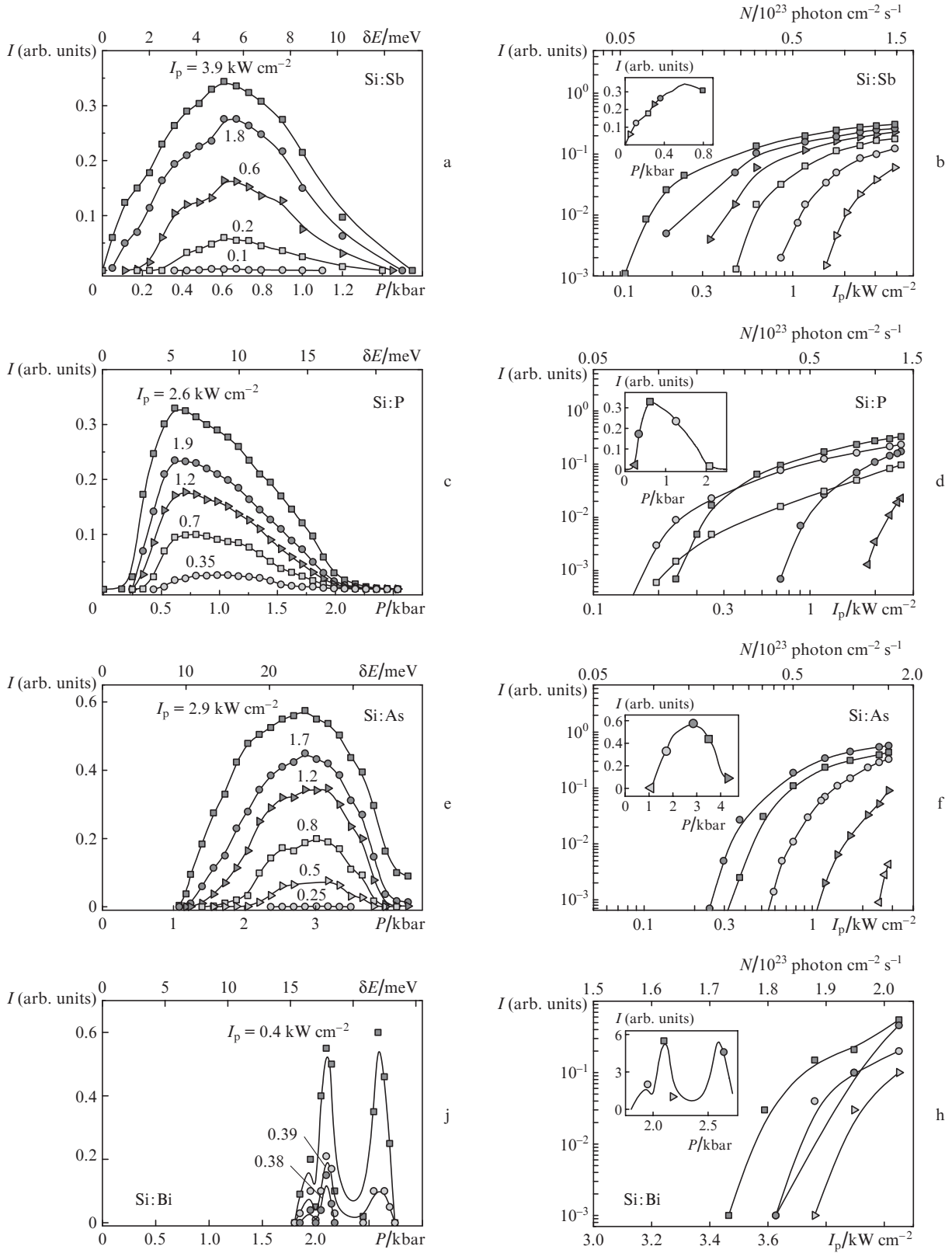
Figure 8. Output stimulated THz emission intensity (a, c, e, g) as a function of [100] compressive strain at the specified pump intensities and (b, d, f, h) as a function of CO_2 laser pump intensity I_p (10.6 μm, 300 ns) at the strain values specified in the insets for group V donors in Si.

the most similar in stimulated emission conditions. Nevertheless, Sb has a lower pump threshold ($I_{th} \approx 100$ W cm^{-2}) at a strain $\delta E_{opt} \approx 5$ meV. These parameters for P are 200 W cm^{-2} and 10 meV, respectively. Note that the stimulated emission

from the P donor persists at higher strain. These data are in conflict with calculated working state populations (see Fig. 6 and Ref. [19]), which suggest that the optimal strain for Si:Sb should be achieved at $\delta E_{opt} \approx 8$ meV and the optimal strain
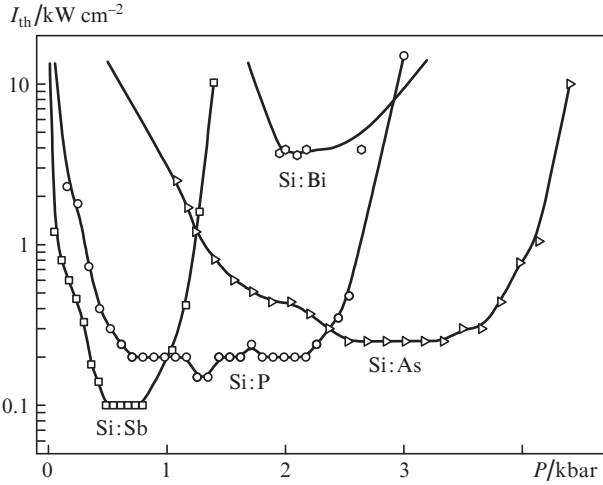
Figure 9. Threshold pump intensity I_{th} as a function of compressive strain ($F\|[100]$) for the Sb, P and As donors in silicon under CO_2 laser excitation ($\lambda = 10.6\ \mu m$, $\tau = 300$ ns). The pump intensity of 2 kW cm^{-2} corresponds to a photon flux density of $\sim 10^{23}$ photon cm^{-2} s^{-1}.

Table 2. Measured and theoretically estimated (*) parameters of silicon THz lasers.

| Parameter	No strain	[100] strain
Gain coefficient:		
$\quad$ photoionisation (10.6 μm)	$\leqslant 0.2$ cm^{-1}	1 cm^{-1} *
$\quad$ intracentre pumping (36 μm)	2–4 cm^{-1}	–
Quantum efficiency:		
$\quad$ photoionisation (10.6 μm)	$\leqslant 1\%$*	$\leqslant 10\%$*
$\quad$ photoionisation (17 μm)	–	$\leqslant 15\%$*
$\quad$ intracentre pumping (19–39 μm)	50%*	–
Efficiency (10.6 μm)	up to 10^{-3} *	up to 10^{-2} *
Threshold pump intensity (10.6 μm)	$\geqslant 15$–100 kW cm^{-2}	$\geqslant 100$–200 W cm^{-2}
Frequency tuning $\Delta\omega/\omega$	0	$\sim 1\%$
Working temperatures	< 15–20 K	
Donor concentration	$(2$–$4)\times 10^{15}$ cm^{-3}	
Lasing frequency range	4.9–6.4 THz	
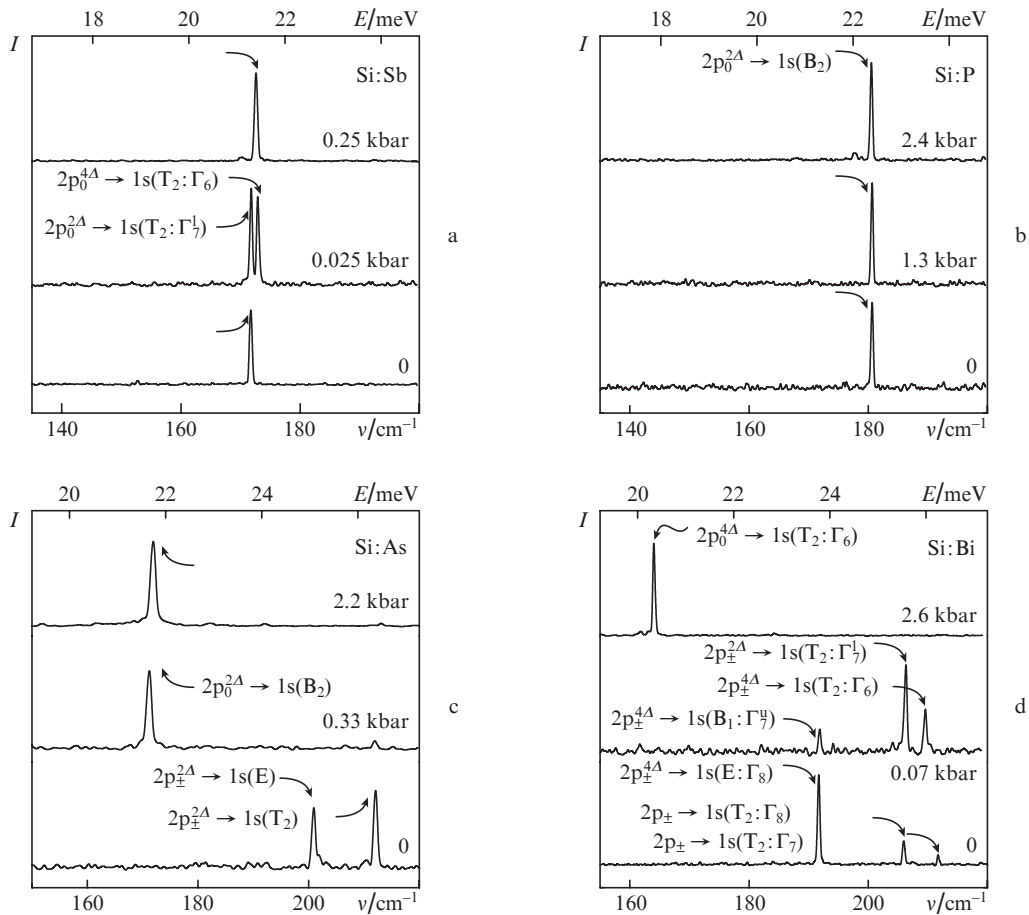
Figure 10. Emission frequencies of group V donors under optical CO_2 laser excitation and uniaxial compressive strain ($F\|[100]$). The numbers at the right-hand vertical axis specify the applied pressure.

for Si:P, at $\delta E_{opt} \approx 5$ meV. We believe that the discrepancy can be partially eliminated by using the parameter $K_0 = 0.85\times 2\pi a^{-1}$ in calculations, whereas the estimate in Fig. 6 was obtained with $K_0 = 0.835\times 2\pi a^{-1}$ [22]. Anyway, perfect quantitative agreement should not be expected, because one should

also take into account parameters other than the working state population and gain. These include the strain dependence of the absorption by negatively charged donors (Figs 4, 5). The same refers to the data for Si:As. Nevertheless, the observed shift to higher optimal strain values for the Sb, P and As
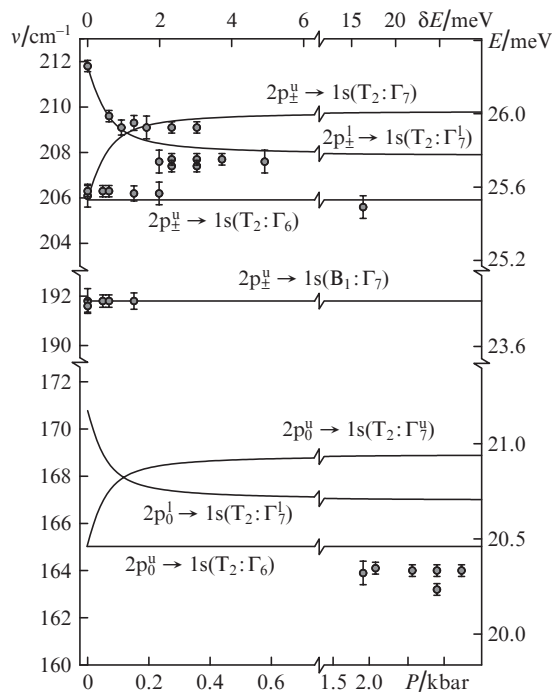
Figure 11. Stimulated emission frequency v as a function of [100] compressive strain for Si : Bi.

donors follows the chemical shift. Recall that the binding energy of the ground state $1s(A_1^l)$ in undeformed silicon is ~42.74 meV for antimony, ~45.59 meV for phosphorus and ~53.76 meV for arsenic [14]. The respective chemical shifts are 11.4, 14.3 and 22.5 meV. According to calculations [12], the lifetime of the lower state $1s(B_2)$ of the working transition is controlled by the interaction with the TA-g intervalley phonons, having an energy of ~12 meV, for the Sb and P donors and with the LA-g and TA-f phonons for the As donor. According to dispersion curves presented in Dolling [26], the energy of such phonons approaches 20 meV. Note that the calculations took into account the chemical shift of the ground state, which was taken to have a hydrogen-like wave function. The detuning of the lower state of the working transition from resonance with the intervalley phonons in question, because of the decrease in the binding energy of the $1s(A_1^l)$ state with increasing strain and the associated decrease in the energy of the $1s(B_2) \rightarrow 1s(A_1)$ transition, leads to a gradual decrease in population inversion and complete suppression of lasing.

The measured emission frequencies of the P and Sb donors (Figs 10a, 10b) are well consistent with calculated spectra of states (the spectrum for P is presented in Fig. 1b). The working transitions are easy to identify. The working transition for the centres in question is $2p_0^{2\Delta} \rightarrow 1s(B_2)$, whose frequency is not influenced by uniaxial deformation of the crystal (according to theory and experiment). The two-frequency lasing observed in the case of the antimony donor at low strain is due to the $1s(T_2 : \Gamma_7^l)$ and $1s(T_2 : \Gamma_6)$ states, which result from the spin–orbit splitting of the $1s(T_2)$ state (Fig. 1a). The measured Sb lasing frequency as a function of strain confirms the estimated spin–orbit coupling parameter $\Lambda_{SO} \approx 0.29$ meV [15]. Like in the case of P, spin–orbit coupling for As atoms is negligible. Therefore, the emission frequency for the transitions indicated in Fig. 10 should be strain-independent (see Fig. 1). At the same time, a change in the binding energy of the $1s(A_1)$

ground state may lead to changes in emission frequencies. This may occur in the case of As, when the crystal is compressed along the [100] axis under a pressure of ~300 bar (Fig. 10c). Frequency switching can be accounted for by the intracentre relaxation of the LA-f intervalley phonon (~47 meV). In undeformed silicon and at low strains, it transfers electrons of the As donor from a 2s state to the $1s(A_1)$ ground state, switching off the pumping of the $2p_0$ state. At the same time, for $P > 300$ bar there is no resonance interaction, and $2p_0$ becomes the most populated excited state. As pointed out above, in undeformed Si : As the $1s(B_2)$ state decays primarily through the emission of LA-g and TA-f intervalley phonons, which are close in energy to the $1s(B_2) \rightarrow 1s(A_1)$ transition. However, at stresses above 1 kbar, these phonons are detuned from resonance, but the relaxation of this state through TA-g phonons becomes important. Therefore, throughout the strain range in question, up to 4–5 kbar (Fig. 6), an inverse population of states and gain on the $2p \rightarrow 1s(B_2)$ transitions should persist.

The measured lasing frequencies as functions of [100] compressive strain for the Bi donor and comparison with the corresponding theoretically predicted behaviour of the spectrum of conduction band states demonstrate that, in contrast to the other group V donors, this centre lases on transitions of the 4Δ valleys under optical excitation at wavelengths in the range $9.6 – 10.6$ µm. This accounts for the observed features of the optimal strain ranges and pump threshold. The ground state energy of the bismuth donor in undeformed silicon is about 71 meV, with a chemical shift of ~39.7 meV. The relaxation of 1s excited states (the lower working states for stimulated emission) is governed by the interaction with the LA-f and LA-g phonons. A significant role in the relaxation of the 2p (upper working) states is played by intervalley transitions caused by interaction with the TO-f and LO-g optical phonons, which determines the specifics of excited state relaxation of this centre [19]. According to spectral measurements in a wide strain range, lasing occurs on transitions of the 4Δ valleys (Fig. 11). The states of the 2Δ valleys have no population inversion because of the direct photoexcited carrier capture from the conduction band to the ground state, accompanied by LO-g phonon emission. There is no such factor in the upper 4Δ valleys. According to measurements, however, only about 10% of the excited electrons reach the working $2p_0^{4\Delta}$ states of the upper valleys, which increases the threshold pump intensity.

6. Output emission directionality and polarisation

Clearly, these characteristics of stimulated emission in the medium under consideration are determined by the cavity design and the strain of the crystal. The corresponding measurements were made using samples in the form of rectangular resonators (Fig. 12a). The emission at zero strain was found to be unpolarised, and its directionality diagram had a large divergence angle: $\theta > 60°$. The use of samples with the shape shown in Fig. 12b allowed us to obtain directional stimulated emission ($\theta \approx 10°$) polarised along the deformation axis. Clearly, this θ value is not a limit and can be further reduced. In particular, this can be achieved by using a silicon coupling prism (Fig. 12c). An additional advantage of such a configuration is the possibility of controlling the stimulated emission output loss by varying the separation between the sample and prism.
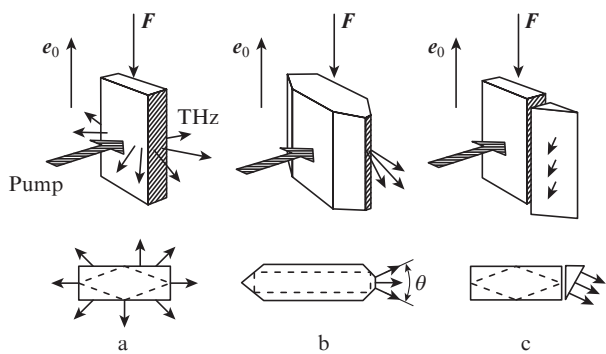
Figure 12. Emission directionality as a function of the shape of the polarisations. The optical field polarisation is $e_0 \| F$.

7. Conclusions

The present results demonstrate that uniaxial compression of a crystal along the [100] axis leads to a considerable increase in the quantum efficiency and gain coefficient of the THz active medium based on donors in silicon under optical CO_2 laser excitation. The threshold pump intensities obtained suggest that quasi-cw lasing is possible. This is the result of the effect of strain on conduction band states, which reduces the internal loss, improves the pump efficiency and decreases the working state relaxation/decay rate. Note also the decrease in internal loss due to the absorption by negatively charged donors and their complexes. Varying the strain may cause not only changes in working transitions (Si:As) and the associated sharp change in lasing frequency but also a more gradual frequency tuning, related to the effect of strain on the spin–orbit splitting of the $1s(T_2)$ states (Si:Bi and Si:Sb).

References

1. Shastin V.N. *21st Int. Conf. on Infrared and Millimeter Waves: Conf. Digest* (Berlin, 1996) abstr. ID CT2.
2. Pavlov S.G., Zhukavin R.Kh., Orlova E.E., Shastin V.N., Kirsanov A.V., Hübers H.-W., Auen K., Riemann H. *Phys. Rev. Lett.*, **84**, 5220 (2000).
3. Pavlov S.G., Hübers H.-W., Rümmeli M.H., Zhukavin R.Kh., Orlova E.E., Shastin V.N., Riemann H. *Appl. Phys. Lett.*, **80**, 4717 (2002).
4. Hübers H.-W., Pavlov S.G., Riemann H., Abrosimov N.V., Zhukavin R.Kh., Shastin V.N. *Appl. Phys. Lett.*, **84**, 3600 (2004).
5. Pavlov S.G., Hübers H.-W., Hovenier J.N., Klaassen T.O., Carder D.A., Phillips P.J., Redlich B., Riemann H., Zhukavin R.Kh., Shastin V.N. *Phys. Rev. Lett.*, **96**, 037404 (2006).
6. Pavlov S.G., Hübers H.-W., Hovenier J.N., Klaassen T.O., Riemann H., Abrosimov N.V., Notzel N., Zhukavin R.Kh., Shastin V.N. *J. Lumin.*, **121**, 304 (2006).
7. Pavlov S.G., Hübers H.-W., Böttger U., Zhukavin R.Kh., Shastin V.N., Hovenier J.N., Redlich B., Abrosimov N.V., Riemann H. *Appl. Phys. Lett.*, **92**, 091111 (2008).
8. Pavlov S.G., Böttger U., Hovenier J.N., Abrosimov N.V., Riemann H., Zhukavin R.Kh., Shastin V.N., Redlich B., van der Meer A.F.G., Hübers H.-W. *Appl. Phys. Lett.*, **94**, 171112 (2009).
9. Pavlov S.G., Böttger U., Eichholz R., Abrosimov N.V., Riemann H., Shastin V.N., Redlich B., Hübers H.-W. *Appl. Phys. Lett.*, **95**, 201110 (2009).
10. Pavlov S.G., Hübers H.-W., Orlova E.E., Zhukavin R.Kh., Riemann H., Nakata H., Shastin V.N. *Phys. Stat. Sol. (b)*, **235** (1), 126 (2003).
11. Tsyplenkov V.V., Kovalevsky K.A., Shastin V.N. *Fiz. Tekh. Poluprovodn.*, **42** (9), 1032 (2008).
12. Tsyplenkov V.V., Kovalevsky K.A., Shastin V.N. *Fiz. Tekh. Poluprovodn.*, **43** (11), 1450 (2009).
13. Bir G.L., Pikus G.E. *Symmetry and Strain-Induced Effects in Semiconductors* (New York: Wiley, 1974; Moscow: Nauka, 1972).
14. Ramdas A.K., Rodriguez S. *Rep. Prog. Phys.*, **44**, 1297 (1981).
15. Mayur A.J., Dean Sciacca M., Ramdas A.K., Rodriguez S. *Phys. Rev. B*, **48** (15), 10893 (1993).
16. Pavlov S.G., Hübers H.-W., Orlova E.E., Zhukavin R.Kh., Shastin V.N. *Semicond. Sci. Technol.*, **19**, 465 (2004).
17. Beinikhes I.L., Kogan Sh.M. *Zh. Eksp. Teor. Fiz.*, **93**, 285 (1987).
18. Oliveira L.E., Falicov L.M. *Phys. Rev. B*, **33**, 6990 (1986).
19. Tsyplenkov V.V. *Cand. Sci. Diss.* (Nizhnii Novgorod: Inst. Physics of Microstructures, Russ. Acad. Sci., 2010).
20. Abakumov V.N., Perel V.I., Yassievich I.N. *Nonradiative Recombination in Semiconductors* (Amsterdam: North-Holland, 1991; St. Petersburg: PIYaF im. B.P. Konstantinova, 1997).
21. Jacoboni C., Reggiani L. *Rev. Mod. Phys.*, **55** (3), 645 (1983).
22. Yu P.Y., Cardona M. (Eds) *Fundamentals of Semiconductors: Physics and Materials* (Berlin: Springer, 2010, 4th ed.; Moscow: Fizmatlit, 2002).
23. Pavlov S.G., Böttger U., Hübers H.-W., Zhukavin R.Kh., Kovalevsky K.A., Tsyplenkov V.V., Shastin V.N., Abrosimov N.V., Riemann H. *Appl. Phys. Lett.*, **90**, 141109 (2007).
24. Zhukavin R.Kh., Tsyplenkov V.V., Kovalevsky K.A., Shastin V.N., Pavlov S.G., Böttger U., Hübers H.-W., Riemann H., Abrosimov N.V., Nötzel N. *Appl. Phys. Lett.*, **90**, 051101 (2007).
25. Shastin V.N., Zhukavin R.Kh., Kovalevsky K.A., Tsyplenkov V.V., Pavlov S.G., Hübers H.-W. *J. Phys.: Conf. Ser.*, **193**, 012086 (2009).
26. Dolling G. in *Inelastic Scattering of Neutrons in Solids and Liquids* (IAEA, Vienna, 1963) Vol. 2, p. 37.